ARTICLE IN PRESS

Materials Today: Proceedings xxx (xxxx) xxx

Contents lists available at ScienceDirect

Materials Today: Proceedings

journal homepage: www.elsevier.com/locate/matpr

A study on dimensional analysis modeling of crater size during wire electrical discharge turning process by using Buckingham Pi theorem

Gajanan M Naik [a], Maheshwar A Hipparagi [b], Sadashiv Bellubbi [c,*], Abhinaba Roy [d], BN. Anjan [e], S. Ramesh [a], S. Narendranath [f]

[a] Department. of Mechanical. Engineering, RV Institute of Technology and Management, JP Nagar, Bangalore 560076, Karnataka, India
[b] Department of Mechanical Engineering, Hirasugar Institute of Technology, Nidasoshi, Belagavi, 591225 Karnataka, India
[c] Department of Mechanical Engineering, Alva's Institute of Engineering and Technology, Moodbidri, 574225 Mangaluru, Karnataka, India
[d] Department of Mechanical Engineering, The National Institute of Engineering, Mysuru 570008, Karnataka, India
[e] Department of Mechanical Engineering, Aurora's Technological and Research Institute, Hyderabad 500098, India
[f] Department of Mechanical Engineering, National Institute of Technology Karnataka, Surathkal, 575025 Mangaluru, Karnataka, India

ARTICLE INFO

Article history:
Available online xxxx

Keywords:
WEDT
SEM
Buckingham's Pi-theorem
Aluminium 6061
INCONEL 718

ABSTRACT

The investigation on material removal by thermal erosion of discrete spark and vaporization in wire electrical discharge turning process was made to understand the crater size variation on turned components. In this study the modelling is done to establish the relationship between dependent and independent variables through Buckingham's Pi-theorem, to predict the variations of crater diameter depending on physical and thermal properties, subsequently the dimensional model was validated by conducting experiments on wire-electrical discharge turning process for two distinct density variant materials such as Aluminium 6061 and INCONEL 718 super alloys. The density, enthalpy of vaporization, radius of spark, specific heat and other quantities effect on crater diameter have been discussed in this research paper.

Selection and peer-review under responsibility of the scientific committee of 2022 International Conference on Recent Advances in Engineering Materials.

1. Introduction

Wire electrical discharge turning (WEDT) process is considered under the categories of nontraditional machining process in which the erosion of material takes place by an electrical discharge between an electrode and work piece, produces an electric spark. Hence it removes unwanted materials from the component in the form of debris, here only electrically conductive materials can be machined with this process [1]. While machining with Wire-EDT processes the materials removed by means of electric spark generated between the inter-electrode gaps thereby it creates a small crater on the surface of the work piece which leads the higher surface roughness. Therefore, it is essential to achieve a good surface finish after machining, that can be achieved by minimizing the diameter of the crater which is formed during turning.

Abimannan & Samuel [2] have reported the finite element analysis on the formation of crater under WEDT process. According to the investigation data, it was found that by increasing discharge energy the crater diameter increases, which leads to rougher work piece surface. Discharge energy can be minimized by increasing the servo feed, spindle speed and servo voltage. Also, author stimulated the crater diameter by using finite element method with different plasma flushing efficiency. Here, it was observed that the crater diameter estimated is nearly matched with experimental value at 3% of plasma flushing efficiency. Jun et al. [3] investigate the surface integrity and roundness during electrical discharge turning of brass components as a result, good surface finish and roundness could be achieved in the WEDT process. The macro-ridges, surface craters, recast layers, and heat-affected zones were observed, and their sizes were estimated using the SEM. Sachin et al. [4] studied the dimensional analysis, formulating a mathematical model in terms of Pi terms using Buckingham's Pi-theorem between independent and dependent parameters. In order to minimize the error between the experimental values and computed values obtained from a mathematical model. Mangesh and Tatwawadi [5] have developed a directional analysis model by using Buckingham's Pi theorem. The results disclose that the cutting condition and the turning parameters have significant effects on the material removal rate (MRR) and the power con-

* Corresponding author.
E-mail address: bellubbisadashiv@gmail.com (S. Bellubbi).

https://doi.org/10.1016/j.matpr.2022.05.508
2214-7853/
Selection and peer-review under responsibility of the scientific committee of 2022 International Conference on Recent Advances in Engineering Materials.

Please cite this article as: Gajanan M Naik, Maheshwar A Hipparagi, S. Bellubbi et al., A study on dimensional analysis modeling of crater size during wire electrical discharge turning process by using Buckingham Pi theorem, Materials Today: Proceedings, https://doi.org/10.1016/j.matpr.2022.05.508

sumption (PC), while the machining tool and the lubricant have the least impact. The developed dimensional analysis models can be used for selecting the best set of input parameters which improve MRR and reduce power consumption [9].

The current research paper formulates the mathematical model, to predict the factors which influence the crater size; this has been modelled by considering physical and thermal properties of the process to bring out the relationship between the crater size and independent quantities using Buckingham's Pi theorem. The properties have been taken in to account based on the literature, the properties are diameter of crater (D), specific heat capacity (Cp), heat flux (q(r)), discharge energy (E), radius of spark (R), erosion energy (Ee), time (t), constant fraction of total power (Fc), discharge time (te), convective heat transfer co-efficient (hc), initial or ambient temperature (T0), enthalpy of vaporization (Hv), temperature at melting condition (Tm), discharge current (I), temperature at boiling condition (Tb), thermal conductivity (k), discharge voltage (u(t)), latent heat of melting (Lm), latent heat of vaporization (Lv) and density of the material(ρ).

2. Experimentation

Buckingham Pi model was examined by conducting the WEDT experiments on aluminium and INCONEL 718, nickel-based superalloy. The thermal properties and mechanical properties are shown in Table 1. The controlled machining parameters and fixed factors are given in Table 2 and Table 3. Taguchi experimental design detailed in reference [6,10,13–15]. Taguchi design reduces number of experiments and hence, cost and time required for the experimentation [16–17].

Based on the L18 Taguchi's orthogonal array experiments were performed. The work piece surface was polished using a belt grinding machine before the machining process. The work piece was held on the WEDT machine using a turning setup as shown in Fig. 1 [6]. During experiments, work piece is rotated closer to the wire electrode in the dielectric environment. Due to the electric discharge between the electrodes, small quantity of material is removed from work piece. Subsequently, the crater size was evaluated by using scanning electron microscopy (SEM) to compare the obtained results with the analytically modelled mathematical equation from Buckingham Pi theorem.

3. Nondimensionalization

The formulation of a dimensional mathematical model is an important step to predict the crater variation on turned components while machining with WEDT process. In order to analyze the crater size the physical and thermal quantities to be identified and is listed in Table 4. The relationship amongst the quantities of crater diameter which is affecting the machined surface is formulated using dimensional analysis. Therefore, Buckingham's dimensional analysis has been used in this work and it expressed a functional relationship of inputs and output response in the form of a mathematical model [5,7]. This theory is highly significant while defining the dimensionless terms and it is an interdisciplinary field of work, which defines the independent variables to analyze output response [4].

The modelling of dimensional analysis by Buckingham's Pi-theorem was considered, valid dependent and independent quantities with the magnitudes of the base units. In this work, our interest is on crater diameter (D), it is a dependent variable, and also this quantity determines the crater size in a well-defined physical process. The formulated dependent and independent quantities are given in equation (1) and (2) in the form of non-homogeneous and homogeneous equation, respectively. However, the fifteen non-dimensional Pi terms have formed by considering a total number of variables and total numbers of fundamental dimensions from Table 4. The obtained Pi groups have given in equation (3), furthermore, the non-dimensional Pi terms have been evaluated according to Buckingham Pi theorem and also coefficients were calculated by taking dimensional homogeneity into account. Finally, the Pi groups have been evaluated and present in Table 5, thereafter the mathematical model has been derived from the Pi groups and represents in equation (20). Consequently, the effects

Table 1
Thermal and mechanical properties of aluminium and INCONEL 718 [12].

Properties	Aluminium	INCONEL 718
Thermal Conductivity, K(W/m-K)	205	11.4
Melting Temperature, T (K)	933.3	1609
Specific Heat, C(J/kg K)	904	435
Density, ρ (kg/m^3)	2700	8190
Young's Modulus, E (GPa)	69	205
Hardness-Brinell (BHN)	99–101	250–410

Table 2
Process parameters and their levels [6,13].

Parameters	Levels		
	L1	L2	L3
Rotational speed (rpm)	150	250	–
Pulse on time (μs)	108	116	124
Pulse off time (μs)	24	32	40
Servo voltage (V)	18	36	54
Wire feed rate (m/min)	2	4	6
Flushing Pressure (bar)	1.8	2.0	2.2

Table 3
Fixed factors and their magnitude.

Factors	Value
Peak voltage(V)	11
Wire Tension (daN)	06
Servo Feed (mu)	2150
Peak current (A)	12
Wire material	Zinc coated brass (250 μm)
Dielectric fluid	De-ionized water

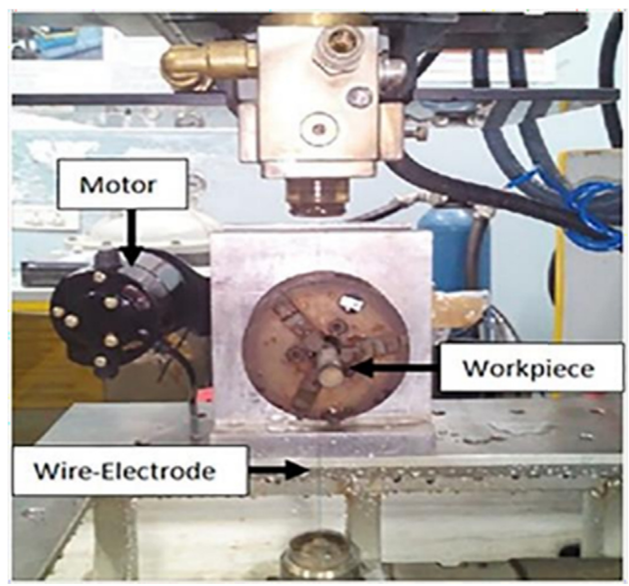

Fig. 1. Experimental setup of WEDT [6].

Table 4
List of Physical and Thermal quantities.

Sl.No	Quantities	Symbol	Units	Dimensions
01	Diameter of crater	D	nm	L
02	Specific heat capacity	C_p	J/kg °c	$L^2T^{-2\theta-1}$
03	Heat flux	q(r)	W/m^2	MT^{-3}
04	Discharge energy	E	J	ML^2T^{-2}
05	Radius of spark	R	µm	L
06	Erosion energy	E_e	J	ML^2T^{-2}
07	Time	t	min	T
08	Constant fraction of total power	F_c	Constant	–
09	Discharge time	t_e	µs	T
10	Convective heat transfer co-efficient	h_c	W/m^2 °c	$MT^{-3\theta-1}$
11	Initial or ambient temperature	T_0	°c	$\theta 1$
12	Enthalpy of vaporization	H_v	J/kg	L^2T^{-2}
13	Temperature at melting condition	T_m	°c	$\theta 1$
14	Discharge current	I	A	QT^{-1}
15	Temperature at boiling condition	T_b	°c	$\theta 1$
16	Thermal conductivity	K	W/m°c	$MLT^{-3\theta-1}$
17	Discharge voltage	u(t)	V	$ML^2T^{-2}Q^{-1}$
18	Latent heat of melting	L_m	J/kg	L^2T^{-2}
19	Latent heat of vaporization	L_v	J/kg	L^2T^{-2}
20	Density of material	ρ	kg/m^3	ML^{-3}

Table 5
Formulation of Pi terms for independent variables.

Sl.No		Pi terms
01	$\pi_1 = R^{a1}Hv^{b1}\rho^{c1}Cp^{d1}u(t)^{e1}D\pi_1 = R^{-1}Hv^0\rho^0Cp^0u(t)^0D$	$\pi_1=\frac{D}{R}$
02	$\pi_2 = R^{a2}Hv^{b2}\rho^{c2}Cp^{d2}u(t)^{e2}q(r)\pi_2 = R^0Hv^{-3/2}\rho^{-1}Cp^0u(t)^0q(r)$	$\pi_2 = \frac{q(r)}{\rho H_v{}^{3/2}}$
03	$\pi_3 = R^{a3}Hv^{b3}\rho^{c3}Cp^{d3}u(t)^{e3}E\pi_3 = R^{-3}Hv^{-1}\rho^{-1}Cp^0u(t)^0E$	$\pi_3=\frac{E}{R^3H_v\rho}$
04	$\pi_4 = R^{a4}Hv^{b4}\rho^{c4}Cp^{d4}u(t)^{e4}E_e\pi_4 = R^{-3}Hv^{-1}\rho^{-1}Cp^0u(t)^0E_e$	$\pi_4 = \frac{E_e}{R^3H_v\rho}$
05	$\pi_5 = R^{a5}Hv^{b5}\rho^{c5}Cp^{d5}u(t)^{e5}t\pi_5 = R^{-1}Hv^{1/2}\rho^0Cp^0u(t)^0t$	$\pi_5 = \frac{tH_v{}^{1/2}}{R}$
06	$\pi_6 = R^{a6}Hv^{b6}\rho^{c6}Cp^{d6}u(t)^{e6}F_c\pi_6 = R^0Hv^0\rho^0Cp^0u(t)^0F_c$	$\pi_6 = F_c$
07	$\pi_7 = R^{a7}Hv^{b7}\rho^{c7}Cp^{d7}u(t)^{e7}t_e\pi_7 = R^{-1}Hv^{1/2}\rho^0Cp^0u(t)^0t_e$	$\pi_7 = \frac{t_eH_v{}^{1/2}}{R}$
08	$\pi_8 = R^{a8}Hv^{b8}\rho^{c8}Cp^{d8}u(t)^{e8}h_c\pi_8 = R^0Hv^{-1/2}\rho^{-1}Cp^{-1}u(t)^0h_c$	$\pi_8 = \frac{h_c}{H_v{}^{1/2}\rho c_p}$
09	$\pi_9 = R^{a9}Hv^{b9}\rho^{c9}Cp^{d9}u(t)^{e9}T_0\pi_9 = R^0Hv^{-1}\rho^0Cp^1u(t)^0T_0$	$\pi_9 = \frac{T_oc_p}{H_v}$
10	$\pi_{10} = R^{a10}Hv^{b10}\rho^{c10}Cp^{d10}u(t)^{e10}T_m\pi_{10} = R^0Hv^{-1}\rho^0Cp^1u(t)^0T_m$	$\pi_{10} = \frac{T_mc_p}{H_v}$
11	$\pi_{11} = R^{a11}Hv^{b11}\rho^{c11}Cp^{d11}u(t)^{e11}I\pi_{11} = R^{-2}Hv^{b-3/2}\rho^{-1}Cp^0u(t)^1I$	$\pi_{11} = \frac{u(t)I}{R^2H_v{}^{3/2}\rho}$
12	$\pi_{12} = R^{a12}Hv^{b12}\rho^{c12}Cp^{d12}u(t)^{e12}T_b\pi_{12} = R^0Hv^{-1}\rho^0Cp^1u(t)^0T_b$	$\pi_{12} = \frac{T_bc_p}{H_v}$
13	$\pi_{13} = R^{a13}Hv^{b13}\rho^{c13}Cp^{d13}u(t)^{e13}k\pi_{13} = R^{-1}Hv^{-1/2}\rho^{-1}Cp^{-1}u(t)^0k$	$\pi_{13} = \frac{k}{RH_v{}^{1/2}\rho c_p}$
14	$\pi_{14} = R^{a14}Hv^{b14}\rho^{c14}Cp^{d14}u(t)^{e14}L_m\pi_{14} = R^0Hv^{-1}\rho^0Cp^0u(t)^0L_m$	$\pi_{14} = \frac{L_m}{H_v}$
15	$\pi_{15} = R^{a15}Hv^{b15}\rho^{c15}Cp^{d15}u(t)^{e15}L_v\pi_{15} = R^0Hv^{-1}\rho^0Cp^0u(t)^0L_v$	$\pi_{15} = \frac{L_v}{H_v}$

of thermal quantities and physical quantities on crater diameter by considering individual parameters in each Pi terms, have been reported in Table 6.

$$D = f\ (C_p, q(r),\ E,\ R,\ E_e, t,\ F_c,\ t_e, h_c,\ T_0,\ H_v,\ T_m,\ I,\ T_b, k,\ u(t),\ L_m,\ L_v,\ \rho) \tag{1}$$

$$f\ (D,\ C_p, q(r),\ E, R,\ E_e, t,\ F_c,\ t_e, h_c,\ T_0,\ H_v,\ T_m,\ I,\ T_b, k,\ u(t),\ L_m,\ L_v,\ \rho) = 0 \tag{2}$$

The total number of quantities identified in the process: n = 20.
The total number of fundamental dimensions involved: m = 5.
The reduced non-dimensional parameter = n-m = 15 Pi terms, Π_1 to Π_{15}.

$$f(\pi_1,\ \pi_2,\ \pi_3,\ \pi_4,\ \pi_5, \pi_6,\ \pi_7,\ \pi_8,\ \pi_9,\ \pi_{10}, \pi_{11}, \pi_{12}, \pi_{13},\ \pi_{14}, \pi_{15}) = 0 \tag{3}$$

The Non-dimensional Pi groups are constructed by taking repeating variables are equal to a number of fundamental dimensions and n-m remaining variables. The value of a_1, b_1, c_1, d_1, e_1 etc is calculated by the principle of dimensional homogeneity.

$$\pi_1 = R^{a1}Hv^{b1}\rho^{c1}Cp^{d1}u(t)^{e1}D \tag{4}$$

$$\pi_2 = R^{a2}Hv^{b2}\rho^{c2}Cp^{d2}u(t)^{e2}q(r) \tag{5}$$

$$\pi_3 = R^{a3}Hv^{b3}\rho^{c3}Cp^{d3}u(t)^{e3}E \tag{6}$$

$$\pi_4 = R^{a4}Hv^{b4}\rho^{c4}Cp^{d4}u(t)^{e4}E_e \tag{7}$$

$$\pi_5 = R^{a5}Hv^{b5}\rho^{c5}Cp^{d5}u(t)^{e5}t \tag{8}$$

$$\pi_6 = R^{a6}Hv^{b6}\rho^{c6}Cp^{d6}u(t)^{e6}F_c \tag{9}$$

$$\pi_7 = R^{a7}Hv^{b7}\rho^{c7}Cp^{d7}u(t)^{e7}t_e \tag{10}$$

$$\pi_8 = R^{a8}Hv^{b8}\rho^{c8}Cp^{d8}u(t)^{e8}h_c \tag{11}$$

Table 6
Dimensional analysis of crater size variation Note: ↑[Increase]: ↓[Decreases].

Quantity (Increasing)	Crater Diameter(D)in nm													
	Π_2	Π_3	Π_4	Π_5	Π_6	Π_7	Π_8	Π_9	Π_{10}	Π_{11}	Π_{12}	Π_{13}	Π_{14}	Π_{15}
C_p							↓	↑	↑		↑	↓		
q(r)	↑													
E		↑												
R	↑	↓	↓		↑		↑	↑	↑	↓	↑		↑	↑
E_e			↑											
T				↑										
F_c					↑									
t_e						↑								
h_c							↑							
T_0								↑						
H_v	↓	↓	↓	↑		↑	↓	↓	↓	↓	↓	↓	↓	↓
T_m									↑					
I										↑				
T_b											↑			
K												↑		
u(t)										↑				
L_m													↑	
L_v														↑
ρ	↓	↓	↓				↓			↓		↓		

$$\pi_9 = R^{a9} Hv^{b9} \rho^{c9} Cp^{d9} u(t)^{e9} T_0 \quad (12)$$

$$\pi_{10} = R^{a10} Hv^{b10} \rho^{c10} Cp^{d10} u(t)^{e10} T_m \quad (13)$$

$$\pi_{11} = R^{a11} Hv^{b11} \rho^{c11} Cp^{d11} u(t)^{e11} I \quad (14)$$

$$\pi_{12} = R^{a12} Hv^{b12} \rho^{c12} Cp^{d12} u(t)^{e12} T_b \quad (15)$$

$$\pi_{13} = R^{a13} Hv^{b13} \rho^{c13} Cp^{d13} u(t)^{e13} k \quad (16)$$

$$\pi_{14} = R^{a14} Hv^{b14} \rho^{c14} Cp^{d14} u(t)^{e14} L_m \quad (17)$$

$$\pi_{15} = R^{a15} Hv^{b15} \rho^{c15} Cp^{d15} u(t)^{e15} L_v \quad (18)$$

$$f(\pi_1, \pi_2, \pi_3, \pi_4, \pi_5, \pi_6, \pi_7, \pi_8, \pi_9, \pi_{10}, \pi_{11}, \pi_{12}, \pi_{13}, \pi_{14}, \pi_{15}) = 0 \quad (19)$$

$$f\left(\frac{D}{R} \; \frac{q}{\rho H_v^{\frac{3}{2}}} \; \frac{E}{R^3 H_v \rho} \; \frac{E_e}{R^3 H_v \rho} \; \frac{t H_v^{\frac{1}{2}}}{R} \; F_c \; \frac{t_e H_v^{\frac{1}{2}}}{R} \; \frac{h_c}{H_v^{\frac{1}{2}} \rho c_p} \; \frac{T_o c_p}{H_v} \; \frac{T_m c_p}{H_v} \; \frac{u(t) I}{R^2 H_v^{3/2} \rho} \; \frac{T_b c_p}{H_v} \; \frac{k}{R H_v^{1/2} \rho\, c_p} \; \frac{L_m}{H_v} \; \frac{L_v}{H_v} \right) = 0.$$

$$\pi_1 = f(\pi_2, \pi_3, \pi_4, \pi_5, \pi_6, \pi_7, \pi_8, \pi_9, \pi_{10}, \pi_{11}, \pi_{12}, \pi_{13}, \pi_{14}, \pi_{15})$$

$$\frac{D}{R} = f\left(\frac{q}{\rho H_v^{\frac{3}{2}}} \; \frac{E}{R^3 H_v \rho} \; \frac{E_e}{R^3 H_v \rho} \; \frac{t H_v^{\frac{1}{2}}}{R} \; F_c \; \frac{t_e H_v^{\frac{1}{2}}}{R} \; \frac{h_c}{H_v^{\frac{1}{2}} \rho c_p} \; \frac{T_o c_p}{H_v} \; \frac{T_m c_p}{H_v} \; \frac{u(t) I}{R^2 H_v^{3/2} \rho} \; \frac{T_b c_p}{H_v} \; \frac{k}{R H_v^{1/2} \rho\, c_p} \; \frac{L_m}{H_v} \; \frac{L_v}{H_v} \right) = 0.$$

$$D = R\left(\frac{q}{\rho H_v^{\frac{3}{2}}} \; \frac{E}{R^3 H_v \rho} \; \frac{E_e}{R^3 H_v \rho} \; \frac{t H_v^{\frac{1}{2}}}{R} \; Fc \; \frac{t_e H_v^{\frac{1}{2}}}{R} \; \frac{h_c}{H_v^{\frac{1}{2}} \rho c_p} \; \frac{T_o c_p}{H_v} \; \frac{T_m c_p}{H_v} \times \frac{u(t) I}{R^2 H_v^{3/2} \rho} \; \frac{T_b c_p}{H_v} \; \frac{k}{R H_v^{1/2} \rho\, c_p} \; \frac{L_m}{H_v} \; \frac{L_v}{H_v} \right) \quad (20)$$

4. Results and discussion

4.1. Analysis of an analytical model derived from Buckingham's Pi theorem

An attempt has made in the mathematical modelling to analyze variations of crater diameter with respect to physical and thermal properties. Table 5 has been shown the obtained Pi terms and equation (20) had given a mathematical model for crater diameter, and also the summary of the analytically modelled data results have been interpreted in Table 6. Now it is necessary to analyze and understand the obtained data from the modelling and this qualitative analysis was made to justify how the real phenomenon influence on the variation of crater size with the interaction of independent Pi terms [8]. From equation (20), it was found that the value of crater diameter varied from four independent variables such as Cp, R, Hv and ρ. By increasing Cp, the crater diameter increases in Π_9, Π_{10} and Π_{12} because of the rise of temperatures such as T_0, Tm and Tb, respectively. Crater diameter decreases in Π_8 and Π_{13} because of density of work-piece and enthalpy of vaporization. The crater diameter increases with increase in spark radius due to high energy supplied into the process but crater size decreases in Π_3, Π_4, Π_{11} because of the enthalpy of vaporization and work piece density. By increasing the enthalpy of vaporization the crater diameter decreases but at Π_5 and Π_7 the crater diameter increases because of machining time and discharge time respectively. By machining denser material can minimize the crater diameter because of high density components are compact, material toughness and rest of all fifteen variables such as q(r), E, E_e, T, Fc, te, hc, To, Tm, I, Tb, k, u(t), Lm, Lv are having direct effect on crater size.

4.2. Validating the analytical modelling with the surface analogy

In order to validate the theoretical model which was derived from the Buckingham's Pi-theorem, the experiments have conducted on two distinct density materials such as Aluminium and INCONEL 718 Nickel based superalloy by using WEDT process, the investigation was carried out according to the Taguchi's L18 Orthogonal array experiments, after machining the turned components surfaces were examined by using Scanning electron microscopy. Selected experimental trial no. 3 for characterization because it shown lower surface roughness [13]. From the observation through SEM, it was found that the crater size is larger on aluminium turned part compared to the INCONEL 718 turned part, as illustrated in the Fig. 1 (a) and (b), respectively. The similar results have been observed by Jun Qu et al. [3] where crater size is larger for material having low density, less hard and low melting point. In addition to that, it is also observed that the crater diameter increases by increasing pulse on time. and by increasing pulse off time crater diameter decreases.

Table 6 presents the summary of independent quantities on crater diameter. Crater size is smaller on higher density material

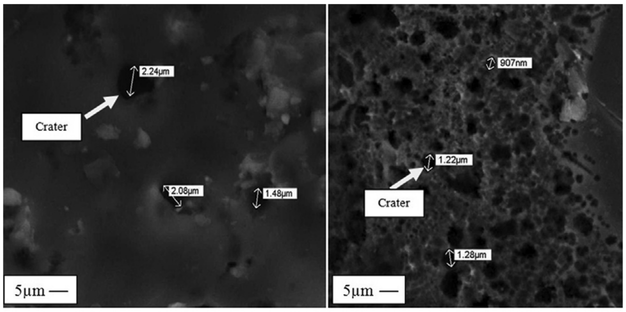

a) Aluminium 6061 b) INCONEL 718

Fig. 2. Surface Micrograph of Aluminium 6061 and INCONEL 718 WEDT component.

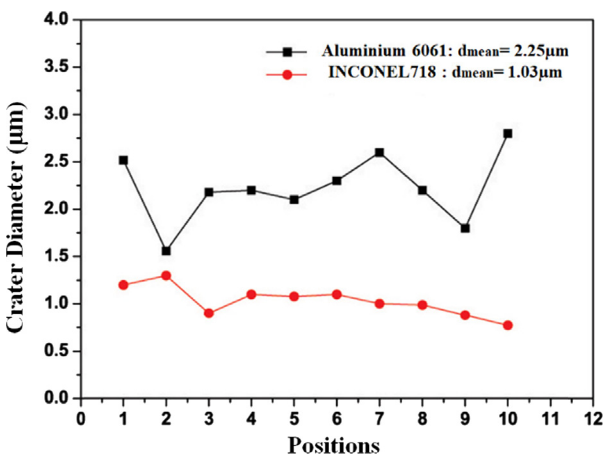

Fig. 3. Mean crater size for Aluminium 6061 and INCONEL 718 WEDT component.

because of high toughness, a similar observation was made by Sharma et al [11] while machining with wire ED machining of INCONEL 706. Fig. 2(a) and (b) shown the crater size information on machined surface of aluminium and INCONEL 718 respectively. From this it is observed that work piece, which is having higher density exhibited lower crater size after machining and it is having good agreement with the published work. Similarly by increasing the enthalpy of vaporization the crater size decreases and specific heat provided an almost neutral effect on crater size and by increasing spark radius the diameter of the crater increases and also remaining variables has been shown a direct effect on crater dimension, that means quantities directly proportional to crater size or crater diameter. The measured mean crater size for aluminium 6061 and INCONEL 718 have shown in Fig. 3. The obtained means crater size for aluminium 6061 and INCONEL 718 is 2.25 μm and 1.03 μm respectively.

5. Conclusions

The Buckingham's Pi-theorem is developed to know the which physical and thermal properties of the process influences more on crater size while machining with WEDT process, according to the Pi theorem and experimental investigations the following conclusion are drawn.

1. The specific heat Cp does not have a major role in the growth of crater diameter; it maintains a neutral effect on the machined surface.
2. The spark radius depends on the supplied current and pulse on time, suppose increasing the supply current and pulse on time the spark radius becomes larger so that the crater formed on the machined surface also large. In order to decrease the crater size, need to operate under low or medium pulse on time condition.
3. The enthalpy of vaporization increases with respect to temperature can minimize the crater size.
4. The materials which are having less density (Aluminum 6061) shown higher crater size on the turned surface compared to denser material (INCONEL718).
5. The properties such as q(r), E, E_e, T, Fc, te, hc, To, Tm, I, Tb, k, u (t), Lm, Lv shows a direct effect on the crater size.

Declaration of Competing Interest

The authors declare that they have no known competing financial interests or personal relationships that could have appeared to influence the work reported in this paper.

References

[1] R.K. Kuldeep Ojha, K.K. Garg, Singh,, MRR Improvement in Sinking Electrical Discharge Machining - A Review, J. Min. Mater. Character. Eng. 9 (2010) 709–739.
[2] Abimannan Giridharan, G.L. Samuel, Modeling and analysis of crater formation during wire electrical discharge turning (WEDT) process, Int. J. Adv. Manuf. Technol. 77 (2015) 1229–1247.
[3] Q.u. Jun, A.J. Shih, R.O. Scattergood, Development of the Cylindrical Wire Electrical Discharge Machining Process, Part 2: Surface Integrity and Roundness, J. Manuf. Sci. Eng. 124 (2002) 708–714.
[4] S.G. Mahakalkar, V.H. Tatwawadi, J.P. Giri, J.P. Modak, The Impact of Dimensional Analysis on Corrugated Sheet Manufacturing Process using Buckingham Pi Theorem, Int. J. Eng. Sci. Innovat. Technol. (IJESIT) 2 (2013) 174–189.
[5] M.R. Phate, V.H. Tatwawadi, Mathematical Models of Material Removal Rate & Power Consumption for Dry Turning of Ferrous Material using Dimensional Analysis in Indian Prospective, Jordan J. Mech. Ind. Eng. 9 (2015) 27–38.
[6] M.N. Gajanan, S. Narendranath, A parametric optimization of Wire-ED Turning process parameters on Material Removal Rate of INCONEL 718, J. Mech. Eng. Biomech. 2 (2) (2017) 8–14, 10/24243/JMEB/.
[7] K. Wang, W. Wang, H. Zhang, J. Fang, "Suction force of vibrating suction method based on pi theorem, Anal. Experiment 86 (2012) 1783–1788.
[8] D.S. Deshmukh, D.C. Talele, M.V. Kulkarni, Development of Mathematical Model for Stationary Compression Ignition Engine Performance Analysis, Int. J. Sci., Spirituality, Bus. Technol 2 (2013) 2277–7261.
[9] S.P. Arikatla, K. Tamil Mannan, A. Krishnaiah, Investigations on Surface Characterisation of Wire Electric Discharge Machined Surface of Titanium Alloy, Int. J. Eng. Res. Technol. 6 (2013) 773–780.
[10] S. Daneshmand, R. Hessami, H. Esfandiar, Investigation of Wire Electro Discharge Machining of Nickel-Titanium Shape Memory Alloys on Surface Roughness and MRR, Life Sci. J. 9 (2012) 2904–2909.
[11] D. Priyaranjan Sharma, S.N. Chakradhar, Evaluation of WEDM performance characteristics of Inconel 706 for turbine disk application, Mater. Des. 88 (2015) 558–566.
[12] Material properties of Inconel 718 from UNS N07718, W. Nr. 2.4668 data sheet.
[13] G.M. Naik, S. Narendranath, Optimization of Wire-ED Turning Process Parameters by Taguchi-Grey Relational Analysis, i-manager's J. Mech. Eng. 8 (2018) 1–8. https://doi.org/10.26634/jme.8.2.14206.
[14] A.S. Shetty, K.S. Akshar, B.Y. Prashanth, G.M. Naik, Optimization of Machining Parameters on MRR for EN19 & EN31 Steel using Taguchi Method, Int. J. Emerg. Res. Manage. Technol. (2017) 2278–9359.
[15] C.J. Vishwas, L.V. Girish, G.M. Naik, B. Sachin, A. Roy, B.Y. Prashanth, R. Badiger, Effect of Machining Parameters on Surface integrity during Dry Turning of AISI 410 martensitic stainless steel, IOP Conf. Series: Mater. Sci. Eng. 376 (2018).
[16] B. Sadashiv, N. Sathisha, B. Mallick, Multi Response Optimization of ECDM Process Parameters for Machining of Microchannel in Silica Glass Using Taguchi–GRA Technique, Silicon (2021) 1–15.
[17] G.M. Naik, B.N. Anjan, R.I. Badiger, S. Bellubbi, D.K. Mishra, An investigation on effects of wire-EDT machining parameters on surface roughness of INCONEL 718, Mater. Today:. Proc. 1 (35) (2021 Jan) 474–477.